JACS
JOURNAL OF THE AMERICAN CHEMICAL SOCIETY

Article

pubs.acs.org/JACS

# Bisboronic Acids for Selective, Physiologically Relevant Direct Glucose Sensing with Surface-Enhanced Raman Spectroscopy

Bhavya Sharma,[‡,†] Pradeep Bugga,[†] Lindsey R. Madison,[†,§] Anne-Isabelle Henry,[†] Martin G. Blaber,[†,∥] Nathan G. Greeneltch,[†,⊥] Naihao Chiang,[†] Milan Mrksich,[†] George C. Schatz,[†] and Richard P. Van Duyne*[,†]

[†]Department of Chemistry, Northwestern University, 2145 Sheridan Rd., Evanston, Illinois 60208, United States

[‡]Department of Chemistry, University of Tennessee, 1420 Circle Dr., Knoxville, Tennessee 37931, United States

Supporting Information

**ABSTRACT:** This paper demonstrates the *direct sensing of glucose at physiologically relevant concentrations* with surface-enhanced Raman spectroscopy (SERS) on gold film-over-nanosphere (AuFON) substrates functionalized with bisboronic acid receptors. The combination of selectivity in the bisboronic acid receptor and spectral resolution in the SERS data allow the sensors to resolve glucose in high backgrounds of fructose and, in combination with multivariate statistical analysis, detect glucose accurately in the 1−10 mM range. Computational modeling supports assignments of the normal modes and vibrational frequencies for the monoboronic acid base of our bisboronic acids, glucose and fructose. These results are promising for the use of bisboronic acids as receptors in SERS-based *in vivo* glucose monitoring sensors.

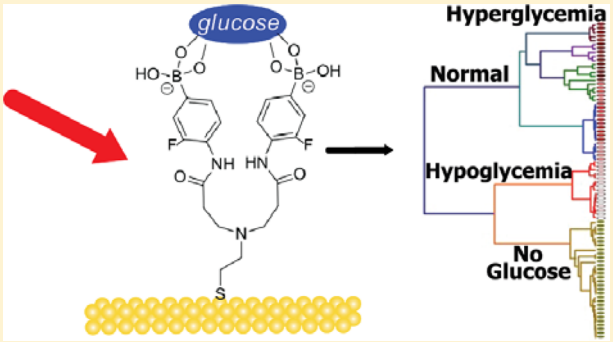


## INTRODUCTION

Diabetes is acknowledged as one of the great health problems facing the 21st century with more than 420 million adults worldwide living with this metabolic disorder.[1] It is estimated that by the year 2050, one in three American adults will be diagnosed with diabetes. With the increasing incidence of diabetes, there is also a large economic cost, due to direct costs of treatment, as well as indirect costs, such as time lost from work. Management of healthy blood glucose levels and minimizing complications will benefit from accurate, passive, and continuous glucose monitoring systems. The gold standard for blood glucose monitoring is the electrochemical test strip and meter system. This method, which relies on indirect detection of enzymatic byproducts, requires frequent monitoring of blood glucose using fingersticks to obtain the blood sample. It is recommended that patients test their blood sugar 8−10 times per day; but due to the pain and inconvenience associated with fingersticks, patient compliance is low. Additionally, a drawback of discrete measurement of blood glucose levels at a few selected times is the possibility for patients to simply miss hypo- or hyperglycemic episodes occurring between two blood checks.

Two challenges facing diabetes researchers are the development of continuous glucose monitoring (CGM) and non-invasive testing methods. On the United States market, the Food and Drug Administration (FDA) recently approved two continuous glucose monitors for human use.[2,3] These devices, however, are somewhat invasive, still require two to four fingerstick calibrations per day,[2,3] and the technology is limited as a result of the enzymatic nature of the sensors, which requires them to be replenished after a given amount of time, and results in indirect measurement of glucose levels.

An alternative technique that has shown great promise for development of an *in vivo* glucose sensor is surface-enhanced Raman spectroscopy (SERS). SERS is a highly sensitive and selective vibrational spectroscopy that can easily detect analytes at low concentration, including small biologically relevant molecules.[4−11] The enhancing effect of SERS is accomplished through an optical frequency electric field generated by the collective oscillation of the surface conduction electrons of noble metal nanoparticles after photoexcitation. This electric field decays rapidly from the substrate surface, thus creating a distance dependence for SERS, where the molecule being detected typically has to be within 2 nm of the nanostructured substrate surface.[12] Additionally, for molecules that do not naturally adsorb to the surface, a capture layer can be used to bring the molecule within the sensing volume.

We previously developed a SERS glucose sensor based on a substrate functionalized with a mixed monolayer of decanethiol and mercaptohexanol (DT/MH) as the capture layer.[13] Through combining SERS with a technique known as spatially

**Received:** July 15, 2016
**Published:** September 26, 2016





DOI: 10.1021/jacs.6b07331
J. Am. Chem. Soc. 2016, 138, 13952−13959

offset Raman spectroscopy (SORS), we also demonstrated with this sensor *in vivo*, transcutaneous detection of glucose in rats for 17 days.[14,15] These SERS-based glucose sensors detected hypoglycemia with high accuracy actually exceeding the current International Organization Standard (ISO/DIS 15197) requirements for hypoglycemic detection limits.[14] While the DT/MH sensor shows great promise for *in vivo* glucose sensing, the capture layer lacks selectivity for glucose over other sugars and the speed necessary for a quick sensing response (>5 min).

Boronic acid molecules are known to covalently bond with saccharides by way of their diol moieties. This interaction is rapid and reversible, resulting in the formation of cyclic boronate esters.[16] Many groups have adapted boronic acids for glucose sensing in combination with fluorescence, colorimetry and surface plasmon resonance.[17] In addition, it has been found that scaffolds incorporating a second boronic acid group enable selectivity for glucose over fructose.[17,18] We have incorporated these elements in designing a boronic acid–based SERS sensor capable of binding glucose selectively and at physiological pH. Though the previously synthesized boronic acid scaffolds are incompatible with SERS due to larger Raman scattering cross sections of the molecules themselves and the large distance between the nanoparticle surface and boronic acid, we determined that 4-amino-3-fluorophenylboronic acid satisfies the necessary requirements for a suitable SERS-based glucose receptor. First reported by Asher and co-workers, this boronic acid displays a p$K_a$ of 7.8, making it optimal for in vivo glucose sensing, and contains an amine functional group for facile immobilization.[19] This manuscript describes the synthesis and characterization of gold film-over-nanosphere (AuFON) substrates functionalized with bisboronic acid receptors incorporating two 4-amino-3-fluorophenylboronic acid units for direct and selective SERS detection of glucose under physiological conditions.

## EXPERIMENTAL METHODS

**Materials.** All the chemicals were reagent grade or better and used as purchased. Glucose, fructose, and 4-amino-3-fluorophenylboronic acid were purchased from Sigma-Aldrich (St. Louis, MO). All samples and substrates were prepared using ultrapure water (18.2 MΩ·cm) from a Millipore system (Marlborough, MA).

**SERS Substrates and Instrumentation.** For these measurements, we utilized gold film over nanosphere (AuFON, also described as immobilized nanorod assembly) SERS substrates, which were previously developed in our group and are well characterized.[20,21] Briefly, polished silicon wafers (WaferNet Inc., San Jose, CA) are used as supports for the SERS substrates. Silica microspheres (Bangs Laboratories, Fishers, IN) are diluted to 5% by volume and are drop-cast onto the Si wafer where they self-assemble into a hexagonal close-packed array. A custom thermal vapor deposition system is used to deposit the Au film (~200 nm thick) made from gold pellets (99.999%; Kurt Lesker Co., Clariton, PA) onto the hexagonal close-packed array.

SERS spectra were recorded on a home-built Raman microscope system that utilizes a Nikon Ti–U inverted microscope (Nikon Instruments Inc., Melville, NY) with a Plan Fluor ELWD 20X objective. SERS spectra were excited at 785 nm (Innovative Photonic Solutions, Monmouth Junction, NJ), with measured powers at the sample varying between 17.7 mW (normal Raman measurements) and 222 $\mu$W (SERS measurements). The AuFON substrates are incubated with the boronic acids for 45 min. After incubation, the substrates are rinsed with deionized water to remove any molecule that is not bound to the surface. The rinsed substrates are then incubated in either the glucose or fructose solutions (in phosphate buffer). It has been previously demonstrated that phosphate buffer does not significantly affect the binding constants of boronic acids.[16] After incubation, the substrates were again rinsed to remove any sugar molecules that did not bind with the boronic acid. The samples are briefly air-dried before measurement of the Raman scattering. The Raman scattered light is dispersed with an Acton SP2300i monochromator (Princeton Instruments, Trenton, NJ) and detected using a liquid $N_2$-cooled CCD camera (Spec10, Princeton Instruments, Trenton, NJ). Laser line rejection was achieved with a 785 nm RazorEdge ultrasteep long-pass edge filter (Semrock Inc., Rochester, NY).

**Computational Modeling.** Calculations of the Raman scattering of glucose, fructose, and the 4-amino-3-fluorophenylboronic acid were performed using density functional theory as implemented in the Amsterdam Density Functional (ADF) software package.[22] The structures of glucose and fructose were taken from Mayes et al.[23,24] The initial geometries underwent further relaxation[25] using the Slater type, triple $\zeta$ with polarization (TZP) basis set and the Becke-Perdew (BP86) exchange-correlation (XC) functional.[26,27] Vibrational frequencies were calculated numerically using the harmonic approximation.[28] The BP86 XC functional was chosen because it results in harmonic vibrational frequencies that more closely match experimental results without incorporating a scaling factor.[29] (At all steps, the COSMO-RS implicit solvent parameters for water were used.[30,31])

The resonance Raman scattering spectra were calculated using the AOResponse module in ADF[22,32,33] following the method described by Jensen et al.[34] This method uses the approximations proposed by Lee[35−37] to the Kramers, Heisenberg, and Dirac formulation of Resonance Raman scattering.

The resonance Raman scattering cross section for any particular vibrational mode $p$ is calculated as

$$\frac{\partial\sigma}{\partial\Omega} = \frac{\pi^2}{\varepsilon_0^{\,2}}(\omega - \omega_p)^4 \frac{h}{8\pi c\omega_p}(S_p)\frac{1}{45(1-\exp(-hc\omega_p/k_BT))}$$

where $\omega$ is the frequency of the incident field, $\omega_p$ is the frequency of the $p$th vibrational mode, and the scattering factor, $S_p$, is composed of the isotropic polarizability derivative, $\bar{\alpha}'$, and the anisotropy $\gamma'$.

$$S_p = 45\bar{\alpha}_p'^2 + 7\gamma_p'^2$$

$$\bar{\alpha}_p' = \frac{1}{3}\sum_i (\alpha_{ii}')_p$$

$$\gamma_p' = \frac{1}{2}\sum_{i,j} 3(\alpha_{ij}')_p(\alpha_{ij}')_p - (\alpha_{ii}')_p(\alpha_{ii}')_p$$

Each vibrational transition was broadened with a Lorentzian function that had a 20 $cm^{-1}$ full width at half-maximum, which is consistent with previous work.[38,39]

**Principal Component Analysis and Hierarchical Cluster Analysis.** Principal component analysis (PCA) is a multivariate statistical analysis used to identify relationships between objects and to classify similar objects. The results of PCA provide an approximation to the data set in terms of variable and object patterns. The application of PCA in this example involves the data set containing N spectra of varying concentrations of glucose-bound bisboronic acid. These N spectra are referred to as the objects and each object has K variables containing information about the Raman scattering intensity between 500 and 1800 $cm^{-1}$.[40] The PCA method is an orthogonal transformation that uses singular value decomposition on the data set, X:

$$\mathbf{X} = \mathbf{U}\cdot\mathbf{S}\cdot\mathbf{V}^T$$

The matrix **U** is a column orthogonal, N × K matrix, **S** is a diagonal K × K matrix, the product **U·S**, when ordered from largest to smallest, contains the principle component eigenvalues of the transformation. The matrix $V^T$ is an orthogonal K x K matrix. The rows of **V** are referred to as the eigenvectors and contain information about the spectral patterns observed.[40,41] To rigorously identify which spectra are similar and to what degree, hierarchical cluster analysis (HCA) was performed on the first six principle components of **U·S.** The Ward cosine definition of distance was used in the HCA algorithm to


DOI: 10.1021/jacs.6b07331
J. Am. Chem. Soc. 2016, 138, 13952−13959

**Scheme 1. Bisboronic Acid Synthesis**[a]

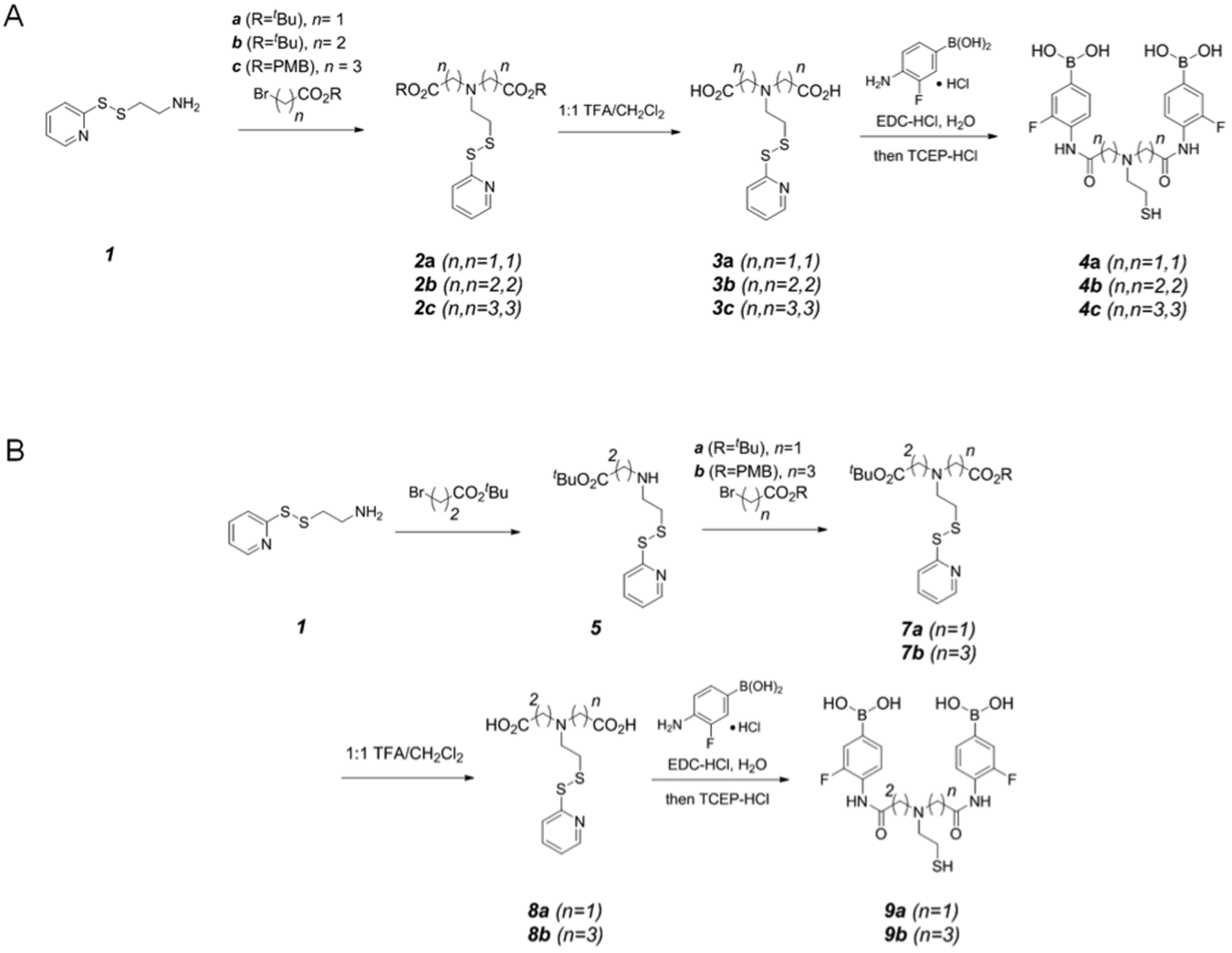


[a](A) Synthesis scheme for 1, 2, and 3 carbon linker bisboronic acid molecules. (B) Synthesis scheme for bisboronic acids with asymmetric carbon linkers (1, 2 and 2, 3). The bisboronic acid molecules contain a chromophore for studying binding with glucose using UV-vis spectroscopy and a thiol for immobilization on SERS substrate.

identify spectra that have eigenvalues that are most similar and to create the dendrogram diagram showing the degree of similarity of the spectra.[41]

## RESULTS AND DISCUSSION

Our approach to developing a physiologically relevant glucose-selective SERS sensor combines the design and synthesis of receptor molecules, computational modeling of the SERS spectra, and surface-enhanced Raman spectroscopy. Before beginning the SERS measurements of glucose and fructose with the boronic acid capture ligands, we first characterized the vibrational modes of these saccharides via normal Raman spectroscopy. As expected, the Raman spectra of solid crystalline sugars and solutions of the sugars (0.5 M) matched the DFT calculated Raman spectra quite well (Supporting Information (SI), Figures S4 and S5). These normal Raman and theory-based calculated spectra allowed us to assign the experimentally observed peaks to specific vibrational modes and to provide some insight into why certain modes of glucose and fructose are visible in the sugar-bound bis-boronic acid spectrum.

In general, sugars do not adsorb to metal surfaces. Therefore, we utilized a receptor to bring them within the sensing distance, i.e., less than 1−2 nm away from the SERS substrate surface.[12] Initially, we used the commercially available monoboronic acid, 4-amino-3-fluorophenylboronic acid to confirm we can detect glucose via a monoboronic acid. We collected SER spectra (Figure S6) of the boronic acid with binding of glucose and fructose. We did not observe discernible changes in the SER spectra of the boronic acid upon binding of the sugars nor did we observe distinct peaks from glucose or fructose. We also used UV−vis spectroscopy to measure the binding affinities of glucose ($K_{gluc} \sim 10\ M^{-1}$) and fructose ($K_{fruc} \sim 200\ M^{-1}$) for the boronic acid. The binding reached equilibrium in less than 1 min (Figures S1 and S2). Considering blood glucose concentrations are ten times that of fructose (5 vs 0.5 mM) and, the binding constant of fructose is 20 times greater than that for glucose, the 4-amino-3-fluorophenylboronic acid molecule does not have any selectivity for glucose over fructose.

To improve the glucose binding affinity and selectivity over fructose, we designed a panel of bisboronic acid sensors with variable length linkers. Shinkai et al. previously demonstrated


DOI: 10.1021/jacs.6b07331
J. Am. Chem. Soc. 2016, 138, 13952−13959

that two boronic acid receptor units are required for achieving specific saccharide selectivity.[18] The high selectivity of bisboronic acids for glucose over other sugars has been further demonstrated by Stephenson-Brown et al., using a surface plasmon resonance-based sensor.[17] Therefore, we employed tertiary amine scaffolds containing two boronic acid arms with variable lengths and a thiol arm for surface immobilization (Scheme 1; full synthesis materials, methods, and characterization in the SI). Importantly, we could construct these sensors expeditiously from sequential alkylation of a protected cysteamine precursor and subsequent 1-ethyl-3-(3-(dimethylamino)propyl) carbodiimide (EDC)-promoted coupling of 4-amino-3-fluorophenylboronic acid. Using the various pairs of readily accessible alkyl bromides allowed us access to the full complement of bisboronic acid analogues.

We again measured the relative glucose and fructose binding affinities via UV−vis spectroscopy for the bisboronic acid analogues (Figure 1, Table 1). Using a phosphate-buffered saline solution having 4% methanol, at a pH of 7.6, we found that the *n*,*n* = 2,2-bisboronic acid provided the largest $K_{glu}$ (167 $M^{-1}$) and also the highest selectivity of glucose versus fructose (0.37).

Our finding that the bisboronic acid analogue with the highest selectivity and affinity contains seven atoms separating the amide carbonyls of the receptor units is consistent with earlier reports by the James and Gibson groups, who separately identified, with their bisboronic acid sensors, that the 6- carbon or 7-carbon linker provides the optimal binding pocket for glucose.[42,43] Finally, all the bisboronic acid analogues displayed higher glucose affinities compared to the 4-amino-3-fluorophenylboronic acid, confirming the cooperative effects of two boronic acid receptor units. We selected the *n*,*n* = 1,1-bisboronic acid (1,1-BBA) molecule for our SERS studies (for *n*,*n* = 1,1, $K_{glu}/K_{fru}$ = 0.10).

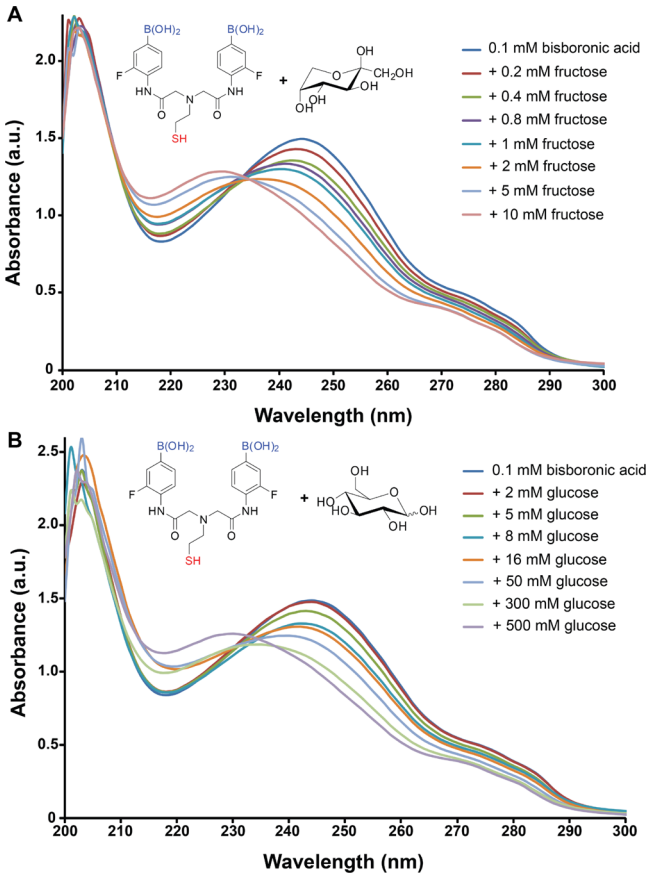


**Figure 1.** UV−vis absorption spectra of the concentration dependent binding of 1,1-BBA with (A) fructose and (B) glucose in 10% MeOH/PBS buffer (pH 7.6). The calculated binding constant for fructose is *K* = 465 $M^{-1}$ and for glucose is *K* = 48 $M^{-1}$.

**Table 1. Glucose and Fructose Selectivity of Bisboronic Acid Analogues**

| | | $K_{glu}$ ($M^{-1}$) | $K_{fru}$ ($M^{-1}$) | $K_{glu}/K_{fru}$ |
|---|---|---|---|---|
| 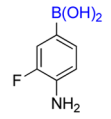 | 4-amino-3-fluoro-phenyl-boronic acid | 10 | 200 | 0.05 |
| 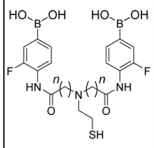 | *n*, *n* = 1, 1 | 48 | 465 | 0.10 |
| | *n*, *n* = 1, 2 | 114 | 389 | 0.29 |
| | *n*, *n* = 2, 2 | 167 | 447 | 0.37 |
| | *n*, *n* = 2, 3 | 99 | 1047 | 0.095 |
| | *n*, *n* = 3, 3 | 29 | 379 | 0.077 |

The vibrations of the boronic acid molecule are outlined in Table 2, and include the predominant vibrations at 1645 $cm^{-1}$ for the in-plane ring stretch (st) with H−N−H bending (b); 1355 $cm^{-1}$ C−B st, ring st, $NH_2$ rock; 1322 $cm^{-1}$ in-plane ring st, N−C st, O−B−O asymmetric st; 906 $cm^{-1}$ ring st; and 787 $cm^{-1}$ ring st.

The physiological levels of glucose concentrations include: hypoglycemia (<4 mM), normal (4−8 mM), and hyper-

**Table 2. Calculated and Experimental Vibrational Modes and Frequencies for 4-Amino-3-fluorophenylboronic Acid**

| calcd ($cm^{-1}$) | exptl ($cm^{-1}$) | mode assignments |
|---|---|---|
| 1645 | 1615 | in-plane, ring st, H−N−H b |
| 1447 | 1434, 1436 | asym. ring b (very weak in calculation) |
| 1355 | 1371 (shoulder) | C−B st, ring st, $NH_2$ rock |
| 1346 | 1344 | C−B−O asym. st, ring st, $NH_2$ rock |
| 1322 | 1339 | in-plane ring st, N−C st, O−B−O asym. st |
| 1187 | weak activity | H (ring) in-plane wave, F−C st |
| 1098 | weak activity | H−O−B b; H (ring) in-plane wave |
| 906 | 909 | ring st |
| 787 | 773 | ring st |
| 684 | 687 | C−B st; ring st, O−B−O b |
| 575 | 600−590 (shoulder) | amine umbrella mode, ring planarity distortion |
| 565 | 600−590 (shoulder) | O−B−O b with amine umbrella mode; out of plane distortions |
| 538 | 571 | O−B−O b, $NH_3$ umbrella; out of plane distortions |
| 528 | 487 | O−B−O b, $NH_3$ umbrella |



DOI: 10.1021/jacs.6b07331
J. Am. Chem. Soc. 2016, 138, 13952−13959

glycemia (>8 mM). To initially test our bisboronic acid sensor, we acquired SER spectra on AuFONs functionalized with the 1,1-BBA molecule, incubated in fructose and glucose at 10 mM concentration (Figures 2 and 3, respectively). Visual inspection

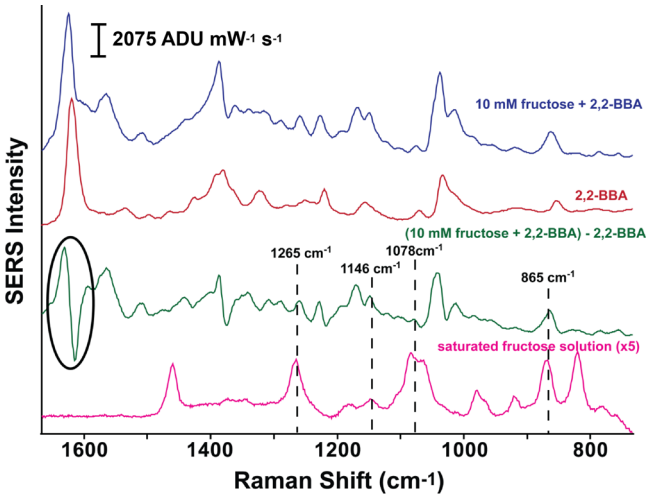


**Figure 2.** SERS spectra of 10 mM (blue) fructose bound to 1,1-BBA on a AuFON, 1,1-BBA on AuFON (red), difference spectrum of (fructose +1,1-BBA) − (1,1-BBA) (green). SERS spectra excited at $\lambda_{ex}$ = 785 nm, $t$ = 5 s, $P$ = 222 $\mu$W; normal Raman spectrum excited at $\lambda_{ex}$ = 785 nm, $t$ = 30 s, $P$ = 17.7 mW.

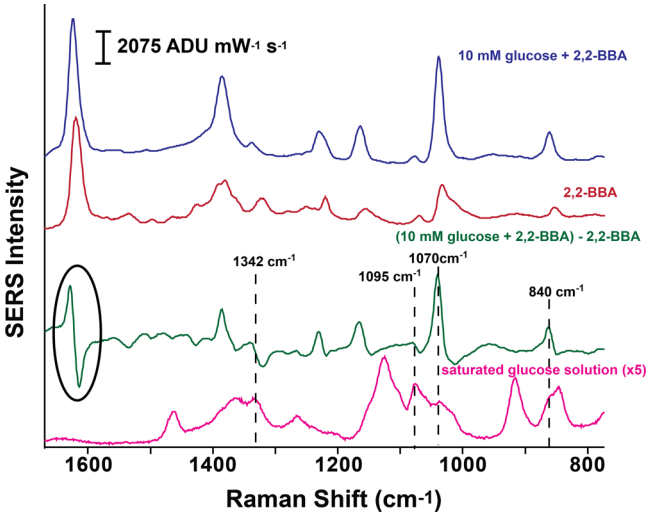


**Figure 3.** SERS spectra of 10 mM (purple) glucose bound to 1,1-BBA on a AuFON, 1,1-BBA on AuFON (red), difference spectrum of (glucose +1,1-BBA) − (1,1-BBA) (green), and the normal Raman spectrum of saturated glucose (pink). SERS spectra excited at $\lambda_{ex}$ = 785 nm, $t$ = 5 s, $P$ = 222 $\mu$W; normal Raman spectrum excited at $\lambda_{ex}$ = 785 nm, $t$ = 30 s, $P$ = 17.7 mW.

of the SER spectra for 1,1-BBA in the presence (Figure 2, blue spectrum) or absence of fructose (Figure 2, red spectrum) as well as that for the receptor in the presence and absence of glucose (Figure 3, blue and red spectra, respectively) revealed little difference between the spectra of the mixed sugar-bisboronic acid spectrum and the bisboronic acid alone. The third spectrum in both figures (green) is a difference spectrum, where the spectrum of 1,1-BBA (red) is subtracted from the spectrum of the sugar with 1,1-BBA (blue).

Difference spectroscopy is a common technique in Raman spectroscopy to elucidate differences in spectra not easily seen by eye. The first remarkable difference is in the boronic acid peak at ~1620 cm$^{-1}$. In the difference spectrum, this peak has a first derivative shape. This distinctive line shape indicates that upon binding of the sugar to the 1,1-BBA, the in-plane ring st, H−N−R b vibration is significantly perturbed, resulting in a shift of the representative bisboronic acid peak by ~5 cm$^{-1}$. Similarly, the derivative-like feature at 1342 cm$^{-1}$ is also attributed to a perturbation of the bisboronic acid (Table 2). Additionally, when comparing the difference spectrum to the spectrum of a saturated sugar solution (pink), it is clear that the ~1095, 1070, and 840 cm$^{-1}$ peaks (highlighted by the dashed lines in Figures 2 and 3) arise directly from the sugar itself. The solid, saturated solution, and calculated spectra of glucose allows us to accurately assign experimentally determined Raman peaks (Table S1). While indirect sensing of glucose is commonly demonstrated with Raman spectroscopy,[13−15,44,45] this is the first *direct* measurement of low concentration sugars demonstrated with SERS.

We further determined that the AuFON 1,1-BBA functionalized glucose sensor is able to detect glucose concentrations in the normal physiological range, as well as hyper- and hypoglycemic concentrations. For difference spectroscopy of each concentration between 1 and 10 mM, we observed both the ~1620 cm$^{-1}$ derivative peak and the characteristic glucose peaks present in the difference spectra (Figure 4). Figure 4

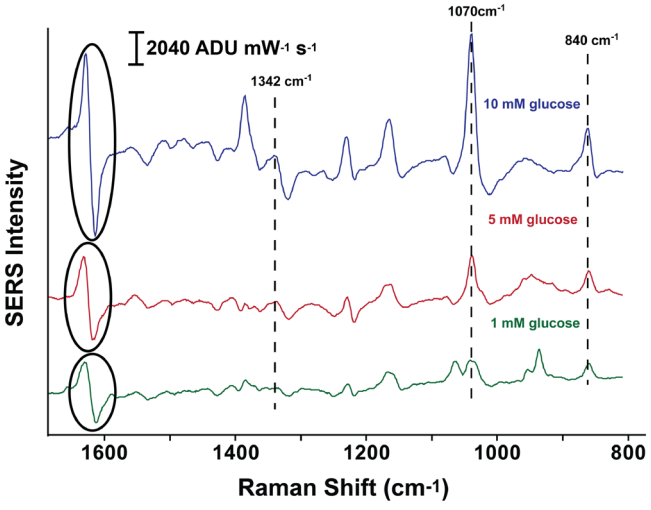


**Figure 4.** SERS difference spectra of 10 mM (blue), 5 mM (red), and 1 mM (green) glucose bound to 1,1-BBA on AuFONs; glucose peaks are indicated by the black dashed lines. SERS spectra excited at $\lambda_{ex}$ = 785 nm, $t$ = 5 s, $P$ = 222 $\mu$W.

clearly demonstrates a direct correlation between the intensities of the 1070 and 840 cm$^{-1}$ peaks and the glucose concentration. Similarly, the amplitudes of the derivative-like features at 1620 and 1342 cm$^{-1}$ are directly correlated with the glucose concentration. When we plot the log concentration dependence of the glucose versus integrated intensity of the 1070 cm$^{-1}$ peak in the difference spectra, which arises from the glucose, we obtain a linear plot with a Pearson's product-moment correlation coefficient r = 0.92, suggesting a strong correlation between the glucose concentration and SERS integrated intensity (Figure 5).


DOI: 10.1021/jacs.6b07331
J. Am. Chem. Soc. 2016, 138, 13952−13959

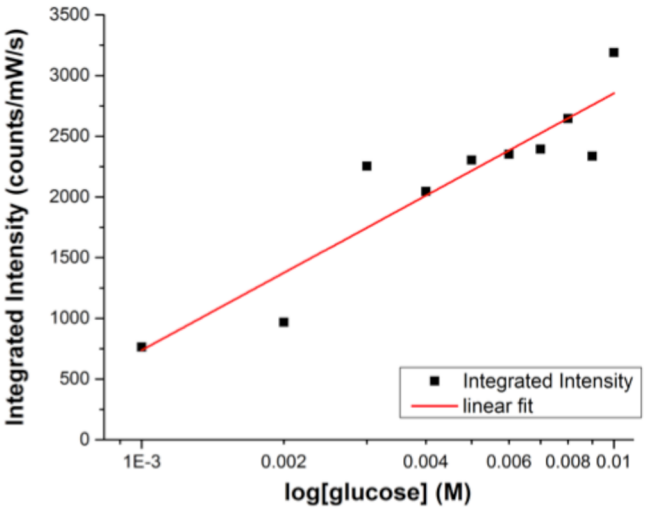


**Figure 5.** Log scale glucose concentration (1−10 mM) versus integrated SERS intensity of the 1070 $cm^{-1}$ peak from concentration dependent SERS difference spectra.

A necessary feature for any glucose sensor is the ability to discriminate between hypoglycemia, hyperglycemia, and normal blood sugar levels. By incorporating principal component analysis (PCA) with our SERS data, we can demonstrate this important capability with our bisboronic acid sensor. PCA is a multivariate statistical method used to classify similar objects. For comparing complicated Raman spectra with small changes in features, such as slight shifts in peak position, PCA is useful in establishing the relationships between spectra. The results of PCA provide an approximation of patterns found between samples probed. We applied PCA to the data set containing N spectra of varying concentrations of glucose-bound bisboronic acid and find that in a comparison of the first principal component (PC1) and the second (PC2) (Figure 6, top left), we obtain clustering of the data into distinct groups. The clustering, however, does not divide the data into discrete concentration groups. To rigorously identify which spectra are similar and to what degree, hierarchical cluster analysis (HCA) was performed on the first six principle components. The HCA algorithm identifies which spectra have highly similar eigenvalues and groups them into a dendrogram diagram that shows the degree of similarity between the spectra. It is important to emphasize that the PC and HC analyses are conducted without incorporating the *a priori* knowledge of the glucose concentrations of the sample and clustering is due to only the similarity between spectra. The HCA diagram clearly breaks down the data into distinct groups of no glucose, hypoglycemia, normal blood sugar, and hyperglycemia. The combined PCA/HCA method can be used to categorize the spectrum of an unknown sample as hypoglycemic, normal, or hyperglycemic. These data indicate the robustness of the AuFON functionalized with 1,1-BBA in sensing different concentrations of glucose.

Finally, to demonstrate the selectivity of our sensor for glucose over fructose we measured the SERS spectra of an equimolar (5 mM) mixture of glucose and fructose. We compared the difference spectrum with the normal Raman spectra of saturated solutions of glucose and fructose (Figure 7). We again observe the distinctive derivative peak centered at 1620 $cm^{-1}$, which is indicative of the sugars binding to the 1,1-BBA (Figure 7, circled peak). We also find that the peaks

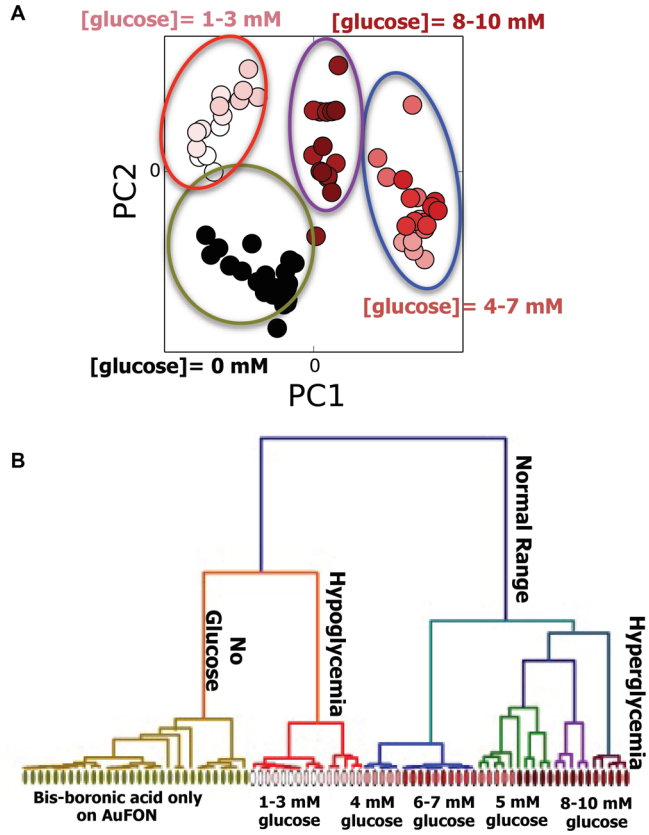


**Figure 6.** PCA comparison of PC1 vs PC2 for varying concentrations of glucose (1−10 mM). Greater distinction between spectra can be found when we couple HCA with PCA. With the HCA we can distinguish between hypoglycemia (1−3 mM), normal (4−8 mM), and hyperglycemia (>8 mM).

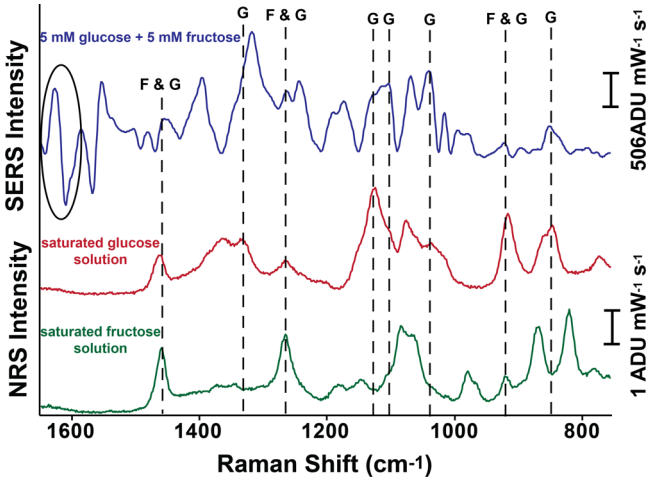


**Figure 7.** SERS difference spectrum of a 5 mM glucose and 5 mM fructose mixture (purple), the normal Raman spectra of a saturated glucose solution (red) and fructose (green). The dashed lines indicate peaks in the SERS spectrum that arise from glucose or fructose. SERS spectrum excited at $\lambda_{ex}$ = 785 nm, $t$ = 5 s, $P$ = 222 $\mu$W; normal Raman spectrum excited at $\lambda_{ex}$ = 785 nm, $t$ = 30 s, $P$ = 17.7 mW.

present in the difference spectrum that arise primarily from glucose, with three peaks that can be attributed to an overlap between glucose and fructose vibrations.

We demonstrated the proof-of-concept and feasibility of a bis-boronic acid−based glucose sensor in the physiologically


DOI: 10.1021/jacs.6b07331
J. Am. Chem. Soc. 2016, 138, 13952−13959

relevant range using SERS. This is the first step toward translating this nanosensor to a platform enabling in vivo, real-time glucose readings. To do so, we plan to collect more data points to define the glucose response, particularly in the low concentration range, and to perform more studies on the selectivity toward glucose, particularly in complex biofluids. Finally, evaluating the long-term response behavior in stringent *ex vivo* media in preparation for in vivo SERS measurements will be paramount in translating this nanosensor to preclinical studies in small animals.

## CONCLUSIONS

We designed and tested multiple bisboronic acid analogues for increased sensitivity in sensing glucose over fructose with SERS. Based on UV−vis absorption data, we determined that the 1,1-BBA analogue was the most well-suited among other analogues (mono- and bisboronic acids with symmetric or asymmetric linkers) for increased glucose sensitivity. Using SERS difference spectra, we showed for the first time, direct sensing of glucose with SERS in the physiologically relevant concentration range. Applying multivariate statistical analysis methods to our data provided increased evidence for the robustness of our sensor in glucose sensing, with clear distinction of the spectra into hypoglycemic, normal, and hyperglycemic ranges. These results are promising for the further development of an in vivo SERS-based glucose sensor.

## ASSOCIATED CONTENT

### Supporting Information

The Supporting Information is available free of charge on the ACS Publications website at DOI: 10.1021/jacs.6b07331.

Synthesis and characterization (UV−visible, NMR) of the bisboronic acid ligands; experimental and calculated spectra of the normal Raman spectra of glucose and a table with the vibrational modes outlined; UV−vis absorption spectra of the 4-amino-3-fluorophenylboronic acid molecule binding glucose and fructose; experimental and calculated normal Raman spectra of the 4-amino-3-fluorophenylboronic acid molecule; and SERS spectra of 4-amino-3-fluorophenylboronic acid binding glucose and fructose (PDF)

## AUTHOR INFORMATION


### Corresponding Author

*vanduyne@northwestern.edu

### Present Addresses

[§]L.R.M.: Department of Chemistry, University of Washington, Box 351700, Seattle, WA 98195−1700.

[∥]M.G.B.: Seagate Technology, 7801 Computer Ave., Bloomington, MN 5543

[⊥]N.G.G.: Intel Corporation, 5200 NE Elam Young Pkwy, Hillsboro, OR 97124


### Notes

The authors declare no competing financial interest.

## ACKNOWLEDGMENTS

This work was supported by the Defense Advanced Research Projects Agency under Grant N660001-11-1-4179 and Cooperative Agreement HR0011-13-2-0002.

## REFERENCES


(1) World Health Organization, Geneva, Switzerland, 2016.
(2) http://www.medtronicdiabetes.com/products/continuous-glucose-monitoring.
(3) https://www.dexcom.com/dexcom-g4-platinum-share.
(4) Graham, D.; Goodacre, R. *Chem. Soc. Rev.* **2008**, *37*, 883.
(5) Granger, J. H.; Schlotter, N. E.; Crawford, A. C.; Porter, M. D. *Chem. Soc. Rev.* **2016**, *45*, 3865.
(6) Henry, A.-I.; Sharma, B.; Cardinal, M. F.; Kurouski, D.; Van Duyne, R. P. *Anal. Chem.* **2016**, *88*, 6638.
(7) Laing, S.; Gracie, K.; Faulds, K. *Chem. Soc. Rev.* **2016**, *45*, 1901.
(8) Schlücker, S. *Angew. Chem., Int. Ed.* **2014**, *53*, 4756.
(9) Sharma, B.; Frontiera, R. R.; Henry, A.-I.; Ringe, E.; Van Duyne, R. P. *Mater. Today (Oxford, U. K.)* **2012**, *15*, 16.
(10) Sonntag, M. D.; Klingsporn, J. M.; Zrimsek, A. B.; Sharma, B.; Ruvuna, L. K.; Van Duyne, R. P. *Chem. Soc. Rev.* **2014**, *43*, 1230.
(11) Stiles, P. L.; Dieringer, J. A.; Shah, N. C.; Van Duyne, R. P. *Annu. Rev. Anal. Chem.* **2008**, *1*, 601.
(12) Masango, S. S.; Hackler, R. A.; Large, N.; Henry, A.-I.; McAnally, M. O.; Schatz, G. C.; Stair, P. C.; Van Duyne, R. P. *Nano Lett.* **2016**, *16*, 4251.
(13) Lyandres, O.; Shah, N. C.; Yonzon, C. R.; Walsh, J. T.; Glucksberg, M. R.; Van Duyne, R. P. *Anal. Chem.* **2005**, *77*, 6134.
(14) Ma, K.; Yuen, J. M.; Shah, N. C.; Walsh, J. T.; Glucksberg, M. R.; Van Duyne, R. P. *Anal. Chem.* **2011**, *83*, 9146.
(15) Yuen, J. M.; Shah, N. C.; Walsh, J. T.; Glucksberg, M. R.; Van Duyne, R. P. *Anal. Chem.* **2010**, *82*, 8382.
(16) *Boronic Acids in Saccharide Recognition*; James, T. D.; Phillips, M. D.; Shinkai, S., Eds.; Royal Society of Chemistry: Cambridge, UK, 2006.
(17) Stephenson-Brown, A.; Wang, H.-C.; Iqbal, P.; Preece, J. A.; Long, Y.; Fossey, J. S.; James, T. D.; Mendes, P. M. *Analyst* **2013**, *138*, 7140.
(18) James, T. D.; Sandanayake, K. R. A. S.; Shinkai, S. *Angew. Chem., Int. Ed. Engl.* **1994**, *33*, 2207.
(19) Das, S.; Alexeev, V. L.; Sharma, A. C.; Geib, S. J.; Asher, S. A. *Tetrahedron Lett.* **2003**, *44*, 7719.
(20) Greeneltch, N. G.; Blaber, M. G.; Henry, A.-I.; Schatz, G. C.; Van Duyne, R. P. *Anal. Chem.* **2013**, *85*, 2297.
(21) Greeneltch, N. G.; Blaber, M. G.; Schatz, G. C.; Van Duyne, R. P. *J. Phys. Chem. C* **2013**, *117*, 2554.
(22) te Velde, G.; Bickelhaupt, F. M.; Baerends, E. J.; Fonseca Guerra, C.; van Gisbergen, S. J.; Snijders, J. G.; Ziegler, T. *J. Comput. Chem.* **2001**, *22*, 931.
(23) Mayes, H. B.; Broadbelt, L. J.; Beckham, G. T. *J. Am. Chem. Soc.* **2014**, *136*, 1008.
(24) Zhou, X.; Nolte, M. W.; Mayes, H. B.; Shanks, B. H.; Broadbelt, L. J. *Ind. Eng. Chem. Res.* **2014**, *53*, 13274.
(25) Kadantsev, E. S.; Klooster, R.; de Boeij, P. L.; Ziegler, T. *Mol. Phys.* **2007**, *105*, 2583.
(26) Becke, A. D. *Phys. Rev. A: At., Mol., Opt. Phys.* **1988**, *38*, 3098.
(27) Perdew, J. *Phys. Rev. B: Condens. Matter Mater. Phys.* **1986**, *33*, 8822.
(28) Fan, L.; Ziegler, T. *J. Chem. Phys.* **1992**, *96*, 9005.
(29) Neugebauer, J.; Hess, B. A. *J. Chem. Phys.* **2003**, *118*, 7215.
(30) Louwen, J. N.; Pye, C. C.; van Lenthe, E.; McGarrity, E. S.; Xiong, R.; Sandler, S. I.; Burnett, R. I. *ADF2014 COSMO-RS, Software for Chemistry & Materials*; Vrije Universiteit: Amsterdam, 2014; http://www.scm.com.
(31) Pye, C. C.; Ziegler, T.; van Lenthe, E.; Louwen, J. N. *Can. J. Chem.* **2009**, *87*, 790.
(32) Baerends, E. J.; Autschbach, J.; Bérces, A.; Bo, C.; Boerrigter, P. M.; Cavallo, L.; Chong, D. P.; Deng, L.; Dickson, R. M.; Ellis, D. E.; Fan, L., . *Amsterdam density functional. Theoretical Chemistry*; Vrije Universiteit: Amsterdam, 2013; http://www.scm.com.
(33) Fonseca Guerra, C.; Snijders, G. J.; te Velde, G.; Baerends, J. E. *Theor. Chem. Acc.* **1998**, *99*, 391.
(34) Jensen, L.; Zhao, L. L.; Autschbach, J.; Schatz, G. C. *J. Chem. Phys.* **2005**, *123*, 174110.




DOI: 10.1021/jacs.6b07331
*J. Am. Chem. Soc.* 2016, 138, 13952−13959

(35) Heller, E. J.; Sundberg, R.; Tannor, D. *J. Phys. Chem.* **1982**, *86*, 1822.
(36) Lee, S.-Y.; Heller, E. J. *J. Chem. Phys.* **1979**, *71*, 4777.
(37) Tannor, D. J. *J. Chem. Phys.* **1982**, *77*, 202.
(38) Aquino, F. W.; Schatz, G. C. *J. Phys. Chem. A* **2014**, *118*, 517.
(39) Mullin, J.; Schatz, G. C. *J. Phys. Chem. A* **2012**, *116*, 1931.
(40) Wold, S.; Esbensen, K.; Geladi, P. *Chemom. Intell. Lab. Syst.* **1987**, *2*, 37.
(41) Press, W. H.; Teukolsky, S. A.; Vetterling, W. T.; Flannery, B. P. *Numerical Recipes: The Art of Scientific Computing*; 3rd ed.; Cambridge University Press, New York, 2007.
(42) Appleton, B.; Gibson, T. D. *Sens. Actuators, B* **2000**, *65*, 302.
(43) Arimori, S.; Bell, M. L.; Oh, C. S.; Frimat, K. A.; James, T. D. *J. Chem. Soc., Perkin Trans.1* **2002**, 803.
(44) Kong, K. V.; Ho, C. J. H.; Gong, T.; Lau, W. K. O.; Olivo, M. *Biosens. Bioelectron.* **2014**, *56*, 186.
(45) Kong, K. V.; Lam, Z.; Lau, W. K. O.; Leong, W. K.; Olivo, M. *J. Am. Chem. Soc.* **2013**, *135*, 18028.


DOI: 10.1021/jacs.6b07331
*J. Am. Chem. Soc.* 2016, 138, 13952−13959